Development 137, 3439-3448 (2010) doi:10.1242/dev.055392

FGF8 acts as a classic diffusible morphogen to pattern the neocortex

Reiko Toyoda[1], Stavroula Assimacopoulos[1], Jennifer Wilcoxon[1], Albert Taylor[1], Polina Feldman[1], Asuka Suzuki-Hirano[2], Tomomi Shimogori[2] and Elizabeth A. Grove[1,*]

SUMMARY

Gain- and loss-of-function experiments have demonstrated that a source of fibroblast growth factor (FGF) 8 regulates anterior to posterior (A/P) patterning in the neocortical area map. Whether FGF8 controls patterning as a classic diffusible morphogen has not been directly tested. We report evidence that FGF8 diffuses through the mouse neocortical primordium from a discrete source in the anterior telencephalon, forms a protein gradient across the entire A/P extent of the primordium, and acts directly at a distance from its source to determine area identity. FGF8 immunofluorescence revealed FGF8 protein distributed in an A/P gradient. Fate-mapping experiments showed that outside the most anterior telencephalon, neocortical progenitor cells did not express *Fgf8*, nor were they derived from *Fgf8*-expressing cells, suggesting that graded distribution of FGF8 results from protein diffusion from the anterior source. Supporting this conclusion, a dominant-negative high-affinity FGF8 receptor captured endogenous FGF8 at a distance from the FGF8 source. New FGF8 sources introduced by electroporation showed haloes of FGF8 immunofluorescence indicative of FGF8 diffusion, and surrounding cells reacted to a new source of FGF8 by upregulating different FGF8-responsive genes in concentric domains around the source. Reducing endogenous FGF8 with the dominant-negative receptor in the central neocortical primordium induced cells to adopt a more posterior area identity, demonstrating long-range area patterning by FGF8. These observations support FGF8 as a classic diffusible morphogen in neocortex, thereby guiding future studies of neocortical pattern formation.

KEY WORDS: Patterning, Neocortex, FGF8, FGF17, Area specification, Mouse

INTRODUCTION

Mammalian neocortex is divided into scores of functionally specialized and anatomically distinct areas that form a consistent area map in each species. Thus, the neocortical area map represents the fundamental way in which the perceptual, cognitive and behavioral functions of the neocortex are organized (Nauta and Feirtag, 1986). Furthermore, although aspects of an area map are species specific, the overall layout of primary sensory and motor areas is conserved across species (Krubitzer, 1995). How the neocortical area map is generated is therefore an important problem in neural patterning. A conceptually simple model (Wolpert, 1996), proposed for patterning diverse developing tissues, would be that classic diffusible morphogens establish initial positional values in the neocortical primordium, which are then read off as different area fates. The best current candidates for such morphogens in neocortex are secreted signaling molecules that belong to the fibroblast growth factor 8 (FGF8) subfamily of FGFs (Ornitz and Itoh, 2001), which have been implicated in patterning the area map along its anterior to posterior (A/P) axis (Dominguez and Rakic, 2008; Grove and Fukuchi-Shimogori, 2003; O'Leary et al., 2007; Sur and Rubenstein, 2005).

Fgf8, *Fgf17* and *Fgf18* are expressed at the anterior pole of the telencephalon (Bachler and Neubuser, 2001; Cholfin and Rubenstein, 2008; Maruoka et al., 1998) at the embryonic stage at which area patterning is initiated (Shimogori and Grove, 2005). FGF17 is required to specify dorsal prefrontal areas but does not have clear effects outside prefrontal cortex (Cholfin and Rubenstein, 2007; Cholfin and Rubenstein, 2008). FGF8, by contrast, has more widespread effects on the neocortical area map. In mice hypomorphic for *Fgf8*, neocortical area boundaries shift anteriorly, towards the depleted source of FGF8 (Garel et al., 2003). Conversely, augmenting the FGF8 source shifts boundaries posteriorly, enlarging anterior areas at the expense of more posterior areas (Fukuchi-Shimogori and Grove, 2001). Most compelling, introducing a second source of FGF8 posteriorly induces mirror-image duplications in the area map (Fukuchi-Shimogori and Grove, 2001).

Several lines of evidence therefore indicate that FGF8 has organizer activity in neocortex. Nonetheless, there have been no direct tests of whether FGF8 meets the criteria for a classic morphogen in the neocortical primordium (Crick, 1970; Driever and Nusslein-Volhard, 1988; Green et al., 1992; Lander et al., 2002; Wolpert, 1969). In this case, FGF8 would form a diffusion gradient along the entire anterior to posterior (A/P) axis of the neocortical primordium, and act directly to impart positional identity, both close to the FGF8 source, and at a distance. An alternative possibility is that FGF8 acts locally to specify area identity and control growth, similar to FGF17. The more extensive effects of FGF8 on area identity would be indirect, mediated by a cascade of other secreted signaling molecules. The two models instigate highly divergent research programs on the cellular and molecular mechanisms that pattern the area map. We therefore sought to test the first model, and to determine whether FGF8 shows features of a classic, diffusible morphogen in the mouse neocortical primordium.

MATERIALS AND METHODS

Mice

Mice carrying null alleles of *Fgf17*, null or hypomorphic alleles of *Fgf8* were obtained from David Ornitz (Washington University) and Anne Moon (University of Utah). InGenious Targeting Laboratory Incorporated generated an *Fgf8*-IRES-Cre mouse, inserting an *IRES-Cre* cassette into

[1]Department of Neurobiology, University of Chicago, Chicago, IL 60637, USA. [2]Shimogori Research Unit, RIKEN Brain Science Institute, 2-1 Hirosawa, Wako City, Saitama 351-0198, Japan.

*Author for correspondence (egrove@bsd.uchicago.edu)

Accepted 3 August 2010

the 3′ end of the *Fgf8* locus immediately downstream of *Fgf8*-coding sequence. Timed pregnant CD-1 mice were obtained from the University of Chicago Transgenic Facility. Noon of the day on which a vaginal plug was seen was termed embryonic day (E) 0.5. Animal use was in accordance with NIH guidelines, and was approved by the University of Chicago IACUC.

Immunohistochemistry

Embryos were fixed in 4% paraformaldehyde and brains sectioned at 10 μm on a Leica CM1830 cryostat. After citrate antigen retrieval, sections were incubated with primary antibody and appropriate HRP-conjugated secondary antibodies. To detect immunofluorescence (IFl), TSA Plus Fluorescence Systems (Perkin-Elmer) was used according to the manufacturer's instructions. Sections were counterstained with 4′,6-diamidino-2-phenylindole, dihydrochloride (DAPI) (Invitrogen) to label cell nuclei and coverslipped with ProLong Gold antifade reagent (Invitrogen).

In situ hybridization

Brains were sectioned at 20 μm with a Leica SM2000R microtome or cryostat sectioned at 10 μm. Single color in situ hybridization (ISH) was as described (Fukuchi-Shimogori and Grove, 2001). Multicolor fluorescence in situ hybridization (FISH) used DIG-, fluorescein (FL)- or 2,4-dinitrophenol (DNP)-labeled ribroprobes. Signal was demonstrated by incubation with FITC, Cy3 or Cy5 tyramide conjugates (Perkin-Elmer). cDNAs were gifts of M. Takeichi (*Cdh6*, *Cdh8*), M. Donoghue (*Efna5*), J. H. Rogers (*Epha7*) and L. F. Reichardt (*p75/Ngfr*). Other riboprobes were obtained with PCR from mouse embryo cDNA.

Cell fate mapping

Fgf8-IRES-Cre mice were crossed with B6-129S4-*Gt(ROSA)26Sor*^{tm1Sor}/J mice (R26R, Jackson Laboratory) to generate progeny carrying both *R26R* and *Fgf8-IRES-Cre* alleles. Cortical cells in the *Fgf8* lineage were identified using a standard X-gal stain for β-galactosidase (Grove et al., 1992).

In utero electroporation

cDNAs encoding mouse FGF8b (Fukuchi-Shimogori and Grove, 2001), other FGFs listed below, a dominant-negative form of human FGF receptor, FGFR3c (dnFGFR3c) and tdTomato (Genove et al., 2005; Nagai et al., 2002; Shaner et al., 2004) were cloned into the pEFX expression vector (Agarwala et al., 2001). PCR primers used to generate the dominant-negative FGFR3c construct from a plasmid containing full-length human *FGFR3c* were: Hs-Fgfr3-F, ATCGCGGCCGCCATGGGCGCCCCTGC-CTG and Hs-Fgfr3-R, ATCGCGGCCGCGGGGGAGCCCAGGCCTTTC. Additional restriction enzyme sites were added to *Fgf8b* and *dnFgfr3c* cDNAs to subclone them in-frame with a *Myc* tag for later immunohistochemical identification. In utero microelectroporation was as described (Fukuchi-Shimogori and Grove, 2001; Shimogori and Ogawa, 2008). tdTomato fluorescence from co-electroporation of *tdTomato* revealed the positions of electroporation sites.

Primary antisera

Antibodies used were: mouse monoclonal against FGF8 (1:5000, R&D Systems, MAB323), with specificity for FGF8 isoforms b and c; mouse monoclonal against human FGF17 (1:10,000, R&D Systems, MAB319); rabbit polyclonal against phospho p44/42 MAP kinase (Thr202/Tyr204) (phospho-ERK) (1:1000, Cell Signaling); rabbit polyclonal against Myc (1:1000, Santa Cruz Biotechnology); mouse monoclonal against Myc (9E10, 1:2000, University of Iowa Hybridoma Bank); and rabbit polyclonal against 5-HTT (1:2000, Immunostar).

Specificity of the mouse monoclonal antibodies against FGF8 and FGF17

By E10.5, FGF2, FGF3, FGF8, FGF15, FGF17 and FGF18 are expressed in the telencephalon (Bachler and Neubuser, 2001; Borello et al., 2008). Thus, specificity of the FGF8 and FGF17 antibodies was crucial to interpretation of immunohistochemical data. To test for cross-reactivity of the FGF8 and FGF17 antibodies with FGF17 and FGF8, respectively, or with FGF2, FGF3, FGF15 and FGF18, the lateral telencencephalon of E10.5 CD-1 embryos was electroporated with mouse *Fgf2* (IMAGE Consortium, clone AI158649), *Fgf3* (Open Biosystems, subsidiary of Thermo Fisher Scientific), *Fgf8* (David Ornitz, Washington University), *Fgf15* (Suzanne Mansour, University of Utah), *Fgf17* (Nobuyuki Itoh, Kyoto University) or human *FGF18* (Open Biosystems). Brains were collected at E11.5 and sectioned into three series. One series was processed with in situ hybridization to identify the *Fgf* electroporation site. The second was processed for FGF8 IFl, and the third for FGF17 IFl. Immunostaining of endogenous FGF8 and FGF17 provided an internal positive control. Neither the MAB323 antibody against FGF8 nor the MAB319 antibody against FGF17 crossreacted with any other FGF tested (n=3 or 4 for each FGF).

Image capture and modification

Images were captured using a Zeiss Axioscope, Axiocam and Axiovision software, or a Leica TCS SP5 laser confocal microscope with LAS-AF software (Leica Microsystems). Deconvolution increased confocal image clarity (Huygens Professional software, Scientific Volume Imaging). For figures, digital images were adjusted for contrast, color and brightness using Adobe Photoshop CS4.

Quantitative analysis of FGF8 immunofluorescence

The gradient of FGF8 IFl intensity in the neocortical primordium at E9.5 was quantified by averaging from light microscopic images of 10 μm sagittal sections near the midline of E9.5 forebrains (one section from each of nine brains). FGF8 IFl is most intense at the midline. Anterior and posterior boundaries of the neocortical primordium were defined, respectively, by the anterior pole of the telencephalon and by an inflection in the neuroepithelium marking the border between neocortical and hippocampal primordia (Altman and Bayer, 1995; Ashwell and Paxinos, 2008; Theiler, 1989). The segment of neuroepithelium in which FGF8 IFl intensities were measured was further standardized for each brain, by setting the width at 25 μm, with the lower edge at the ventricular surface, thereby covering the region where FGF8 IFl is most evident (see Results).

The nine curved neuroepithelial segments were digitally straightened with an established method (Long et al., 2009). Digital straightening allowed samples with varying curvature to be aligned and stacked (ImageJ, series 1.4, NIH, average z-projection routine). This permitted an image of average FGF8 IFl intensities along the A/P length of the neocortical primordium to be generated from the nine samples, and FGF8 IFl intensity to be plotted in arbitrary units (AU, Image J) against A/P distance from the FGF8 source (Fig. 2D). For this plot, the mean IFl intensity through the ventricular to pial width of a segment was calculated at one-pixel A/P intervals. Measurements were obtained from the 'average' segment, or from individual segments, then averaged, with the same results. Similar procedures were used to quantify gradients of FGF8 IFl and pERK IFl in the neocortical primordium at E10.5. Because the neocortex is thicker at E10.5, the segment of neuroepithelium in which IFl intensity was measured was 60 μm in width.

No errors were introduced into IFL intensity measures by the straightening process, which consisted of fitting, by hand, a line following the curve of the neocortical primordium. The ImageJ straightening algorithm fitted a spline to the curved line, with the lower border at the ventricular edge, selected points spaced 1 pixel apart, generated perpendicular lines at each point, and rigidly rotated the perpendicular lines to create the straightened version (Wayne Rasband, ImageJ, NIH). Plotting intensity values at one-pixel intervals along a line down the center of a sample, following its original curved contours, or after straightening, produced essentially identical results (see Fig. S1 in the supplementary material).

RESULTS

If FGF8 is a classic morphogen for the neocortex, FGF8 should form a gradient over the neocortical primordium during the period in which area patterning occurs. Based on previous electroporation experiments in which FGF8 levels were manipulated at different

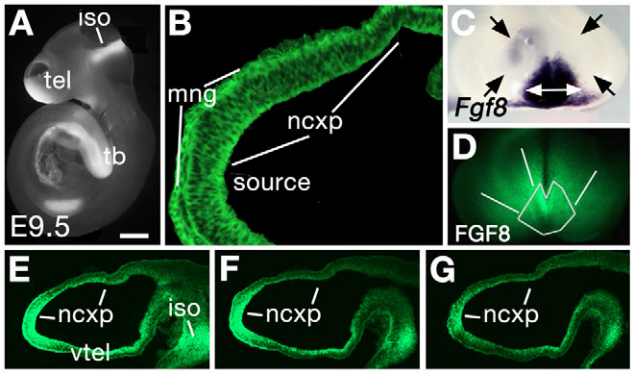

Fig. 1. FGF8 is distributed throughout the neocortical primordium at E9.5. (**A**) E9.5 mouse embryo processed for FGF8-immunofluorescence (IFl). A hole visible in the telencephalon allowed reagent access. FGF8 IFl appears in the tail bud (tb), isthmus (iso) and anterior telencephalon (tel). (**B**,**E-G**) Sagittal brain sections, anterior towards the left, processed for FGF8 IFl. (B) FGF8 IFl extends throughout the neocortical primordium (ncxp). The meninges (mng) also show FGF8 IFl. (E-G) Sagittal sections from medial to lateral (M/L), one brain. FGF8 IFl intensity decreases along A/P and M/L axes. vtel, ventral telencephalon. (**C**,**D**) E9.5 forebrains, frontal view. *Fgf8* expression marks an FGF8 source 200 μm in diameter (C, white double-headed arrow; black arrows indicate ncxp). (D) Gray lines outline the FGF8 source, based on gene expression in C, and indicate FGF8 IFl extending posterior and lateral to the source. Scale bar in A: 0.5 mm for A; 0.03 mm for B; 0.1 mm for C,D; 0.15 mm for E-G.

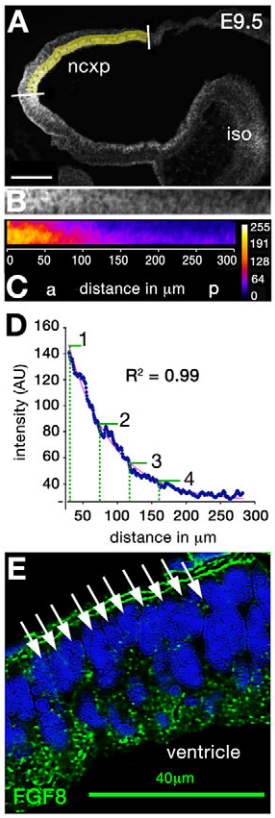

Fig. 2. Characterization of the A/P FGF8 gradient at E9.5. (**A**) Sagittal midline section through one of nine mouse brains used in quantification. FGF8 IFl was measured in a standardized segment of the neocortical primordium (ncxp) (yellow band; white lines mark anterior and posterior ncxp boundaries). The width of the standard segment was set at 25 μm, extending from the ventricular surface. Most FGF8 IFl appears in this 25 μm wide domain, rich in cytoplasm and cell membrane; packed cell nuclei dominate closer to the pial surface (compare A with E). (**B**,**C**) FGF8 IFl (grayscale) in a digitally straightened segment shows an A/P intensity gradient (B), as does FGF8 IFl (false-colored) averaged from nine segments (C). (**D**) Plot of mean FGF8 IFl in arbitrary units (AU) against distance from the anterior FGF8 source. An IFl intensity plateau in the most anterior 25 μm (C) was not plotted in D. A declining exponential curve (red) was fitted to the remaining data (blue). The *x* and *y* axes of the plot in D do not start at zero in order to allow easier identification of sequential half-decline points of the gradient. Maximum FGF8 IFl intensity is (1); sequential half-decline points are labeled (2), (3) and (4). The A/P distance of the half-decline is about 45 μm (see broken green lines in D), roughly the width of 10 DAPI-stained nuclei (white arrows, **E**). Scale bars: 0.1 mm in A; 0.04 mm in E.

embryonic ages, we estimated that initial area patterning begins at about E9.5 in the mouse, and is malleable for a few days (Shimogori and Grove, 2005). At E9.5, the neocortical primordium is still a sheet of dividing cells, a standard developmental stage for morphogen patterning (Echelard et al., 1993; Ericson et al., 1995; Green, 2002; Liem et al., 1995).

FGF8 is distributed throughout the neocortical primordium

Consistent with previous studies (Aoto et al., 2002; Bachler and Neubuser, 2001; Cholfin and Rubenstein, 2008; Crossley and Martin, 1995; Fukuchi-Shimogori and Grove, 2001; Maruoka et al., 1998), strong *Fgf8* gene expression was localized to the anteromedial telencephalon at E9.5, marking the potential source of diffusible FGF8 (Fig. 1C). FGF8 immunofluorescence (IFl) was most intense at this site, and further revealed FGF8 protein throughout the neocortical primordium in a high to low A/P gradient (Fig. 1B,D-G). FGF8 IFl remained widespread in the neocortical primordium, at lower intensity levels, until at least E11.5 (see Fig. S2B in the supplementary material).

An exponentially declining gradient of FGF8

The FGF8 IFl intensity gradient along the A/P axis was quantified from standardized segments of neocortical neuroepithelium from nine brains (Fig. 2A, see Materials and methods for details). Curved segments of neuroepithelium were digitally straightened (Fig. 2B) and stacked to generate an 'averaged' image of the FGF8 IFl gradient, which showed an A/P gradient with an anterior plateau of high intensity (Fig. 2C). Mean IFl values were plotted against A/P distance with the plateau region excluded, and a declining exponential curve (Fig. 2D, red) was fit to the data (Fig. 2D, blue) with ImageJ regression analysis. IFl intensity declined by half over about 45 μm (Fig. 2D, representing about 10 cell widths (Fig. 2E). Given that cells can adopt different fates in response to as little as twofold differences in morphogen concentration (Green and Smith, 1990), the half-decline of FGF8 IFl, compared with the total length of the neocortical primordium at E9.5 (75-80 cell widths, n=9 brains), suggests that several different area fates for a neocortical 'protomap' (Rakic, 1988) could be obtained from the FGF8 gradient we estimate.

In subsequent experiments, FGF8 levels were manipulated with in utero microelectroporation at E10.5; we therefore also assessed the FGF8 gradient at this age. Consistent with observations at E9.5, FGF8 IFl was distributed through the neocortical primordium with an A/P gradient that declined exponentially, following an anterior

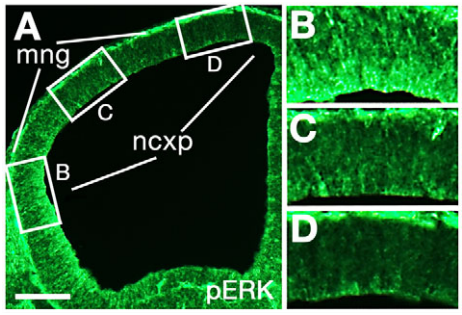

Fig. 3. pERK Ifl is distributed in an A/P gradient at E10.5. (**A**) Sagittal section through an E10.5 mouse brain processed for pERK immunofluorescence. (**B-D**) The boxed areas in A at higher magnification. pERK Ifl declines in intensity from B to C to D. mng, meninges; ncxp, neocortical primordium. Scale bar: 0.120 mm for A; 0.045 mm for B-D.

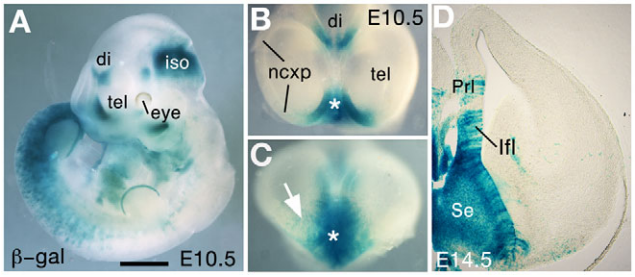

Fig. 4. Few neocortical progenitor cells derive from *Fgf8*-expressing cells. (A-D) Mouse embryos carrying *Fgf8-IRES-Cre* and *R26R* alleles, X-gal-stained. (**A**) In an E10.5 embryo, X-gal staining appears in the anterior telencephalon (tel), dorsal diencephalon (di) and isthmic organizer (iso). (**B**,**C**) E10.5 forebrain in dorsal (B) and frontal (C) views. X-gal labels the FGF8 source (asterisks), and scattered cells in anteromedial neocortical primordium (ncxp) (C, arrow). No X-gal-positive cells appear in dorsal, lateral or posterior ncxp. (**D**) Coronal section of E14.5 telencephalon. X-gal labels cells in the septum (Se), and presumptive infralimbic (Ifl) and prelimbic (Prl) areas, with virtually no labeling elsewhere in the ncxp. Scale bar: 1.0 mm for A; 0.4 mm for B,D; 0.25 mm for C.

plateau of high intensity (see Fig. S3 in the supplementary material). The half decline of the gradient was roughly 100 μm at E10.5, consonant with the A/P growth of the neocortex between E9.5 and E10.5.

Given that growth factors mediated by receptor tyrosine kinases, including FGFs, activate the Ras-extracellular signal-regulated (Ras/ERK) pathway (Schlessinger, 2000), we hypothesized that a gradient of FGF8 would generate a gradient of activated Ras/ERK. Supporting the possibility, phospho-ERK (pERK) IFl at E10.5 showed an A/P gradient in the neocortical primordium (Fig. 3A-D, *n*=6 brains). A caveat in interpreting this finding is that other FGFs in the embryonic telencephalon (Bachler and Neubuser, 2001; Borello et al., 2008) could contribute to – or obscure – a pERK gradient induced by FGF8.

FGF dispersion through the neocortical primordium

Demonstrating a gradient of FGF8 raises the question of how FGF8 distributes across the neocortical primordium. FGF8 may diffuse from a source, as demonstrated in zebrafish (Scholpp and Brand, 2004; Yu et al., 2009), or an *Fgf8* mRNA gradient established as the primordium develops may be translated into an FGF8 protein gradient, as in vertebrate head-to-tail patterning (Dubrulle and Pourquie, 2004). Alternatively, neocortical progenitor cells could inherit FGF8 from their founder cells, a possibility supported by the potential overlap between dorsal telencephalic founder cells and an *Fgf8*-expressing region in the anterior neural fold (Cobos et al., 2001; Sanchez-Arrones et al., 2009).

To evaluate the second two alternatives, we used Cre recombinase mapping to determine the fate of *Fgf8*-expressing cells from the onset of *Fgf8* expression in the embryo, focusing on the specific contribution of the *Fgf8*-lineage to the neocortical primordium. In mice carrying both *Fgf8-IRES-Cre* and *R26R* reporter alleles, cells expressing *Fgf8*, or derived from *Fgf8*-expressing cells, were permanently labeled with *lacZ*. X-gal staining of embryos at E10.5 (*n*=4), accurately reflected the pattern of expression of *Fgf8* in the anterior telencephalon, dorsal diencephalon and isthmic organizer (ISO), and showed expected staining in the body and tail (Fig. 4A). Very little X-gal staining was seen in the neocortical primordium, except in the most anteromedial regions, confirming that *Fgf8* expressing cells and their progeny are confined to the anterior telencephalon at E10.5 (Fig. 4B,C). Coronal sections from E14.5 brains (*n*=4) showed dense X-gal cell labeling in the septal nuclei, and medial prefrontal cortex, but not elsewhere in the neocortical primordium (Fig. 4D). These observations indicate that most neocortical progenitor cells do not express *Fgf8*, nor are they descended from cells that do.

FGF8 dispersion by diffusion from a source

To determine the competency of FGF8 to diffuse through the neocortical primordium, ectopic sources of Myc-tagged FGF8 were introduced at E10.5 by in utero microelectroporation. *Myc-Fgf8* electroporation was aimed towards lateral and posterior cortical primordium, away from the endogenous FGF8 source. Twenty hours after electroporation, Myc-tagged FGF8 was detected by Myc IFl, thereby distinguishing electroporated from endogenous FGF8. Borders of the electroporation site were determined in the same tissue section by tdTomato fluorescence (Fig. 5A), and by ectopic *Fgf8* gene expression in a neighboring section. Brains were selected for a dense electroporation site, about 100-200 μm wide. Myc IFl indicated tagged FGF8 diffusion from each ectopic source reaching more than 30 cell widths (150-200 μm) from the edge of the electroporation site (Fig. 5B,C; *n*=5/5 brains).

A false appearance of FGF8 diffusion could result if *Fgf8* upregulated its own expression during this experiment, generating FGF8 at a distance from the electroporation site. Extensive tangential cell movement from the electroporation site could give the same impression. *Fgf8* and *tdTomato* were co-electroporated at E10.5, and expression of *tdTomato* and *Fgf8* detected at E11.5 in single sections with double FISH. In no case did *Fgf8* expression extend beyond the *tdTomato*-expressing electroporation site (see Fig. S4 in the supplementary material, *n*=6/6 brains, three sections/brain). Furthermore, few labeled cells appeared at a distance from the body of the electroporation site, suggesting minimal tangential cell movement.

Sources of FGF8 induce expression of different target genes at different distances

FGF8 regulates the FGF8 synexpression gene group, which includes Spry genes, encoding negative regulators of FGF8 signaling, and *Pea3/Etv4* and *Erm/Etv5*, encoding Ets transcription

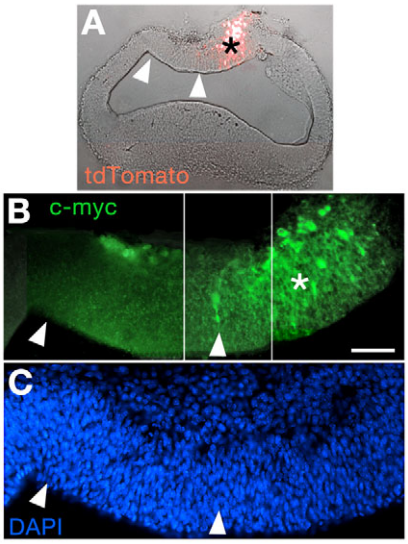

Fig. 5. FGF8 diffuses from electroporation sites of *Fgf8*. (A-C) Sagittal section (anterior towards the left) through a telencephalon, 20 hours after co-electroporation with *Myc-Fgf8b* and *tdTomato* at E10.5. (**A**) Complete section, merged light-field and fluorescence, shows the electroporation site (asterisk). Arrowheads in A-C indicate the same region throughout the figure. (**B**) One continuous image composed of three fields immediately apposed at white lines rather than spliced together. Myc IFl labels cell bodies at the electroporation site (asterisk). Diffuse IFl appears away from the site (between white arrowheads), decreasing with distance. (**C**) DAPI stain of the same section, magnification as in B; the distance between the white arrowheads is roughly 30 cell widths. Scale bar: 0.05 mm for B,C; 0.15 mm for A.

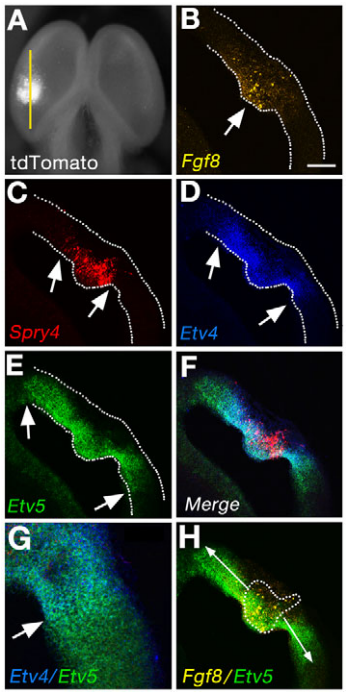

Fig. 6. FGF8 induces expression of different target genes at different distances. (**A**) E11.5 brain, dorsal view, electroporated with *Fgf8b* at E10.5. tdTomato (white) marks the electroporation site; yellow line indicates the position of the sagittal section in C-H, processed for multicolor FISH. (**B**) *Fgf8*-expressing cells at the electroporation site (arrow indicates center) in a section adjacent to C-H. (**C-H**) *Spry4* is expressed at the electroporation site (C), *Etv4* in a larger domain (D) and *Etv5* in a still broader domain (E). Arrows in C-E indicate limits of gene expression. (F) Merge of C-E showing nested gene expression. (G) *Etv4* expression shows a relatively sharp boundary (arrow) suggesting that the gene turns off expression below a specific required level of FGF8. (H) *Etv5* expression extends 100-150 μm (arrows) from the *Fgf8*-expressing electroporation site. Scale bar: 0.5 mm for A; 0.1 mm for B-F,H; 0.03 mm for G.

factors (Niehrs and Meinhardt, 2002). In the mouse telencephalon, Spry genes are expressed anteromedially, close to the source of FGF8, indicating a requirement for high FGF8 levels; *Etv4* and *Etv5* expression domains extend progressively further from the FGF8 source along the A/P axis, suggesting expression of *Etv4* and *Etv5* requires progressively lower levels of FGF8 (Cholfin and Rubenstein, 2008; Fukuchi-Shimogori and Grove, 2003). We took advantage of this nested gene expression pattern to determine whether a new source of FGF8 controls different transcriptional states in cells at different distances from the source, a key prediction for a diffusible morphogen. Electroporation of tagged or untagged *FGF8* at E10.5 was aimed laterally and posteriorly, away from endogenous expression of *Spry4*, *Etv4* and *Etv5*. Multicolor FISH detected sites of *Fgf8* electroporation and *Spry4*, *Etv4* and *Etv5* expression domains at E11.5 (Fig. 6). Recapitulating normal patterns, *Spry4* was expressed close to ectopic FGF8 (Fig. 6B,C,F), *Etv4* was upregulated in a larger domain (Fig. 6D,F), and the *Etv5* expression domain extended furthest from the FGF8 source, encompassing both the *Spry4*- and *Etv4*-expressing territories (Fig. 6E,F). Such nested gene expression patterns, with the same order of specific gene expression domains, formed around new FGF8 sources in nine out of nine brains.

A dominant-negative FGF receptor sequesters FGF8 at a distance from its source

A dominant-negative (dn) FGF receptor, lacking the intracellular tyrosine-kinase signaling domain (Fig. 7A) (Amaya et al., 1991) was generated to determine whether FGF8 acts at a distance from its source to pattern the neocortex. Based on in vitro observations that FGF8 shows a high affinity for FGFR3 isoform c (MacArthur et al., 1995; Ornitz and Itoh, 2001; Ornitz et al., 1996; Zhang et al., 2006) and on results obtained from electroporating a mutant FGFR3c in mouse (Fukuchi-Shimogori and Grove, 2001), the FGFR3c receptor isoform was selected for these experiments. dnFGFR3c was predicted to sequester FGF8 from functional receptors at the electroporation site and thereby reduce FGF8 signaling.

Brains were electroporated with *dnFgfr3c* at E9.5 and processed for double IFl at E10.5 to detect endogenous FGF8 and Myc-tagged dnFGFR3c in the same tissue section. A prominent increase in FGF8-IFl intensity at the *dnFgfr3c* electroporation site showed an accumulation of endogenous FGF8 protein (Fig. 7B-D, n=7/7). Notably, dnFGFR3c sequestered FGF8 outside its anterior source, indicating diffusion of endogenous FGF8 (Fig. 7D,E, right arrows). Furthermore, the higher intensity of FGF8 IFl at the electroporation site compared with the FGF8 source itself (Fig. 7C), suggested that dnFGFR3c efficiently captures FGF8 as more protein diffuses from its source. Confocal microscopy confirmed colocalization of FGF8 and dnFGFR3c at the cell surface (Fig. 7J-M), and revealed FGF8 IFl puncta between electroporated cells (Fig. 7G,H, arrows), reflecting FGF8 that escaped sequestration.

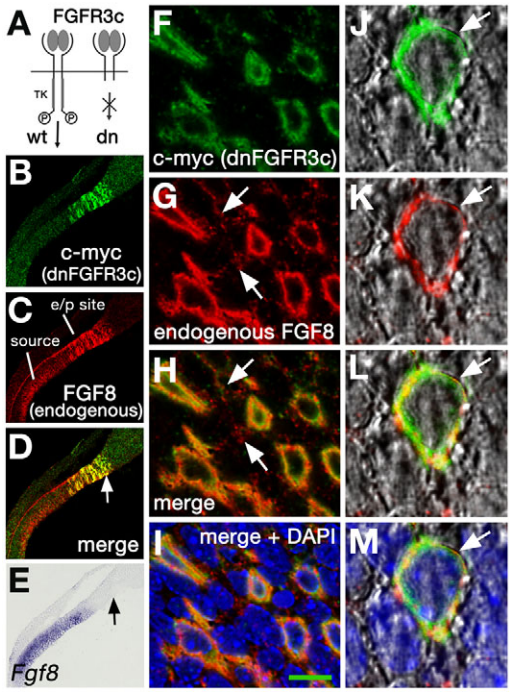

Fig. 7. Dominant-negative FGFR3c sequesters FGF8. (**A**) Schematic wild-type (wt) and dominant-negative (dn) FGFR3c. dnFGFR3c lacks the tyrosine kinase (TK) domain that mediates FGF signaling. (B-M) Confocal images of sagittal sections from an E10.5 brain electroporated at E9.5 with *Myc-dnFgfr3c*. (**B-D**) One section processed for two-color IFl; (**E**) adjacent section processed for in situ hybridization for *Fgf8*. (B-E) DnFGFR3c (green Myc IFl, B) accumulates endogenous FGF8 protein (red IFl, C) (merged image in D), even at a distance from the FGF8 source (right arrows, D,E). (**F-I**) Myc and FGF8 IFl colocalize at the surface of electroporated cells. Punctate FGF8-IFl (white arrows, G,H) indicates FGF8 that escaped sequestration. (**J-M**) Higher magnification reveals colocalization at the cell membrane (white arrows). Scale bar: 0.150 mm for B-E; 0.01 mm for F-I; 0.004 mm for J-M.

Consistent with FGF signal transduction (Cobb and Goldsmith, 1995; Tsang and Dawid, 2004), and previous observations described above, electroporation of *Fgf8* at E9.5 activated the Ras-ERK pathway, indicated by increased pERK IFl at the *Fgf8* electroporation site (see Fig. S5 in the supplementary material, *n*=9/9). Conversely, a large reduction of endogenous pERK IFl at sites of *dnFgfr3c* electroporation confirmed that dnFGFR3c reduces downstream FGF8 signaling (see Fig. S5 in the supplementary material, *n*=12/12). Based on these observations, dnFGFR3c was used to reduce FGF8 signaling at discrete sites in the neocortical primordium, testing the hypothesis that FGF8 acts directly at a distance to determine area identity.

Evidence for long-range area patterning by FGF8

The transcription factor gene *Coup-TF1/Nr2f1* is expressed regionally in the posterior neocortical primordium, plays an important role in area specification (Armentano et al., 2007) and is downregulated by FGF8 (Sansom et al., 2005). Electroporation of *dnFgfr3c* at E10.5 in central/posterior neocortical primordium consistently caused an anterior expansion of the *Nr2f1* expression domain at E13.5, evidently by removing FGF8-mediated inhibition. Anteromedial expression of Ets genes, far from the electroporation sites, was unaffected (see Fig. S6 in the supplementary material, *n*=10/11). These observations imply the ability of FGF8 to act at a distance from its source, in this case inhibiting a gene critical for neocortical patterning. We therefore examined the later effects of E10.5 *dnFgfr3c* electroporation on area gene expression at P0, when gene expression patterns indicate emerging neocortical area boundaries (Fukuchi-Shimogori and Grove, 2001; Garel et al., 2003; Miyashita-Lin et al., 1999; Rubenstein et al., 1999) (*n*=10 brains, central/posterior electroporation verified with tdTomato fluorescence). Sections were processed with in situ hybridization for *p75NTR/Ngfr*, expressed posteriorly, for *ephrinA5/Efna5*, expressed strongly in presumptive primary somatosensory cortex (S1) (Mackarehtschian et al., 1999), and for *Epha7*, which shows a complementary pattern to *Efna5* with both anterior and posterior expression domains (Yun et al., 2003).

In eight out of ten brains, posterior gene expression domains, including *p75NTR/Ngfr*, were expanded anteriorly, with a corresponding reduction of adjacent central domains. These shifts occurred at the *dnFgfr3c* electroporation sites and precisely correlated with the position and size of the sites. For example, *dnFgfr3c* electroporation in ‘brain 2’ extended anterior to that in ‘brain 1’ (Fig. 8B,C,E,F). In both brains, sagittal sections that cut through presumptive S1 in the parietal (Pa) domain, and primary visual cortex (V1) in the occipital (Oc) domain revealed an expanded *Epha7*-expressing Oc domain and a reduced *Efna5*-expressing S1, compared with a control brain (Fig. 8G-L). Brain 2, however, showed a larger anterior expansion of the *Epha7*-expressing Oc domain, and a more shrunken S1 than brain 1, correlating with the anterior borders of the electroporation sites in the two brains. These observations support the hypothesis that reducing FGF8 at discrete locations in the neocortical primordium induces cells to alter their fate and adopt a more posterior area identity.

A formal possibility is that electroporating *dnFgfr3c* affects area patterning by binding to other telencephalic FGFs, such as FGF2, FGF3, FGF15, FGF17 and FGF18 (Mason, 2007). Only FGF8 and FGF17 are implicated in area specification, however (Cholfin and Rubenstein, 2007; Cholfin and Rubenstein, 2008; Fukuchi-Shimogori and Grove, 2001; Garel et al., 2003; Grove and Fukuchi-Shimogori, 2003), and because FGF17 has less influence on overall neocortical patterning than FGF8 (Cholfin and Rubenstein, 2007) (see below), most of the effect of dnFGFR3c on area identity is likely to be mediated by sequestering FGF8.

FGF8 and FGF2 promote telencephalic growth (Borello et al., 2008; Garel et al., 2003; Raballo et al., 2000; Storm et al., 2003); thus, *dnFgfr3c* electroporation might induce differential growth in the cortical primordium, leading to apparent area shifts. This seems an unlikely explanation of present results, given that inhibiting FGF2 and FGF8 would decrease growth at sites of *dnFgfr3c*, leading to effects on area domains opposite to those we observed. In brain 1, for example, the *dnFgfr3c* electroporation site incorporates part of the Oc domain, yet we saw expansion, not shrinkage, of this domain.

FGF17 cooperates with FGF8 to regulate A/P patterning of the neocortex

The chief consequences of *Fgf17* loss are in prefrontal cortex (Cholfin and Rubenstein, 2007), whereas, in mice hypomorphic for *Fgf8*, patterning shifts appear throughout neocortex (Garel et al., 2003). Nonetheless, the entire A/P extent of the neocortical primordium from E9.5 to E11.5 displays FGF17 IFl (see Fig. S2 in the supplementary material), suggesting FGF8 and FGF17

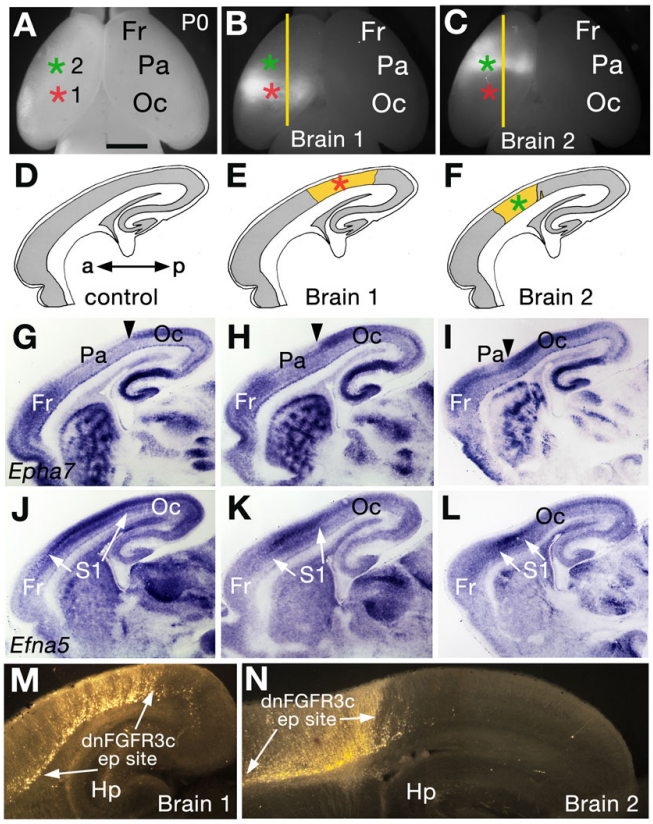

Fig. 8. Electroporation of *dnFgfr3c* induces cells to adopt a more posterior area fate. (**A-C**) Forebrains at P0, dorsal view, anterior is upwards. (A) Non-electroporated brain with cortical domains indicated. Red and green asterisks indicate centers of the *dnFgfr3c* electroporation sites in brains 1 and 2 (A-C,E,F). Yellow lines in B,C indicate section position in H,I,K,L. (**D-F**) Schematic sagittal sections illustrating electroporation sites (yellow) in brains 1 and 2. The site in brain 2 (F) is anterior to that in brain 1 (E). (G-L) Sagittal sections from a control hemisphere (G,J), brain 1 (H,K) and brain 2 (I,L) processed for in situ hybridization. (**G-I**) In the control (G), expression of *Epha7* picks out the Oc and Fr domains. In the control, brain 1 and brain 2, the *Epha7*-expressing Oc domain reaches progressively more anteriorly (arrowheads, G-I). (**J-L**) *Efna5* expression in the control (J) outlines developing S1, which is progressively smaller in brain 1 and brain 2, as central tissue is respecified to a more posterior fate. (**M**,**N**) tdTomato fluorescence documents the extent of each electroporation site in sagittal sections. Close inspection of the anterior boundary of the *dnFgfr3c* electroporation (ep) site in brains 1 and 2 shows near identity with the anterior boundary of the Oc domain, defined by gene expression (compare E,F with M,N and H,I). Abbreviation: Hp, hippocampus. Scale bar: 0.8 mm for A-C; 1.0 mm for D-L; 0.5 mm for M,N.

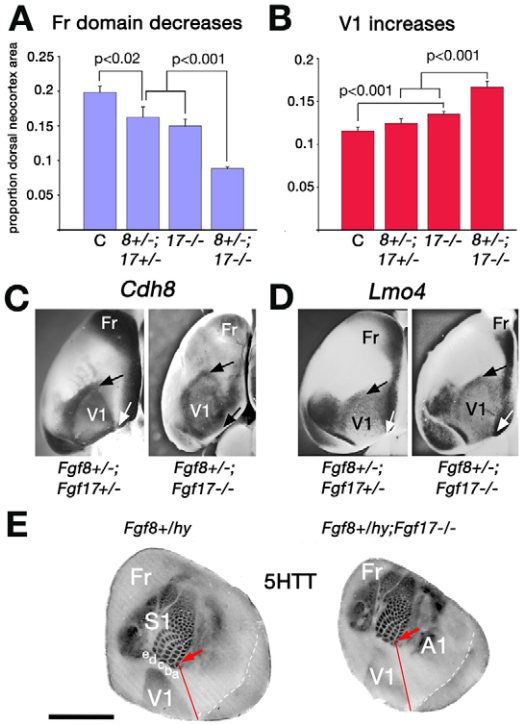

Fig. 9. A/P patterning in neocortex correlates with gene dosage of *Fgf8* and *Fgf17*. (**A**,**B**) Surface areas of the frontal domain (Fr) (A) and V1 (B) as a proportion of total neocortical area in different genotypes. *Fgf8*$^{+/-}$ and *Fgf17*$^{+/-}$ mice showed normal gene expression domains and were included in the control group (c, *n*=10). Fr decreases in proportional area as *Fgf8* and *Fgf17* gene dose falls (A), whereas V1 increases (B). Data are represented as means±s.e.m. (**C**,**D**) P6 hemispheres, dorsal view, anterior is upwards. *Cdh8* and *Lmo4* expression demarcates Fr and the triangular V1. V1 is larger in absolute size in *Fgf8*$^{+/-}$;*Fgf17*$^{-/-}$ brains (right panels, C,D; arrows indicate V1) compared with double heterozygotes (left panels, C,D). (**E**) Sections through P6 flattened cortices, processed for 5HTT-IR. The absolute distance between two posterior landmarks (red lines, arrows) is increased in a *Fgf8*$^{+/hy}$;*Fgf17*$^{-/-}$ brain (right) compared with a control (left). a-e indicate barrel rows in the main barrel field of S1. Scale bar: 2.5 mm for E; 3.0 mm for C,D.

cooperate in patterning. Decreased *Fgf8/Fgf17* gene dose reduces FGF8/FGF17 protein activity (Cholfin and Rubenstein, 2007; Cholfin and Rubenstein, 2008), therefore, if FGF8 and FGF17 act together to pattern the entire neocortex, a progressive decrease in *Fgf8/Fgf17* gene dose should generate progressive posterior to anterior boundary shifts in the area map. An analysis of neocortical area patterning in mice carrying *Fgf17*-null alleles (Xu et al., 1999; Xu et al., 2000), alone or in combination with null or hypomorphic (*hy*) alleles of *Fgf8* (Moon and Capecchi, 2000) supported this hypothesis, and confirmed that FGF8 is the primary agent of the two in overall neocortical patterning.

At P6, *Cdh6*, *Cdh8* and *Lmo4* expression demarcates a neocortical frontal domain (Fr), and primary visual cortex (V1) (Fig. 9C,D). In mice of various genotypes, ImageJ was used to measure the surface areas of Fr, V1 and the entire neocortex, with reference to *Cdh6* and *Lmo4* expression patterns. In *Fgf8*$^{+/-}$;*Fgf17*$^{+/-}$ (*n*=6) or *Fgf17*$^{-/-}$ (*n*=12) mice, the Fr domain decreased, compared with controls (*n*=10), relative to total neocortical surface area (Fig. 9A). V1 appeared proportionally larger in *Fgf17* nulls (Fig. 9B), but this could in principle result from shrinkage of the neocortex caused by reduction of the Fr domain. More compelling changes were seen when a functional *Fgf8* allele was removed from the *Fgf17* null, or an additional *Fgf17* allele from the double heterozygote. The *Fgf8*$^{+/-}$;*Fgf17*$^{-/-}$ genotype (*n*=7) displayed a greatly decreased Fr, and a significantly increased V1 in both proportional and absolute (*P*=0.003) size (Fig. 9A-D). The increase in absolute size of V1 in *Fgf8*$^{+/-}$;*Fgf17*$^{-/-}$ mice is more impressive given that the total neocortical area in these mice is significantly decreased compared with controls (*t*-test, *P*<0.01, *n*=8, each group).

Very little loss of *Fgf8* function is required to see combined effects of *Fgf8* and *Fgf17* depletion. Replacing a functional *Fgf8* allele in the *Fgf17* null with a hypomorphic *Fgf8* allele (50% function) (Frank et al., 2002) expanded posterior neocortical domains. In sections through flattened cortex processed for 5HTT-IR, the absolute length from the posterior edge of the neocortex to a common point in S1 (barrel A1) was greater in $Fgf8^{+/hy};Fgf17^{-/-}$ (n=6) than in $Fgf8^{+/hy}$ mice (n=5) (P=0.03) (Fig. 9E, red lines, arrows), despite a significantly smaller overall neocortical area in the former (P<0.01). $Fgf17^{-/-}$, $Fgf8^{+/-};Fgf17^{+/-}$ and $Fgf8^{+/hy}$ mice showed no significant differences with controls in overall neocortical area at this age (Cholfin and Rubenstein, 2007) (present study). These findings reveal functionally significant levels of both FGF8 and FGF17 in the posterior neocortical primordium that regulate regional specification and tissue growth.

DISCUSSION

FGF8 as a neocortical morphogen

Several lines of evidence indicate that FGF8 diffuses from its source in the anterior telencephalon, forms a gradient from anterior to posterior across the neocortical primordium, and acts at a distance from its source to regulate neocortical area identity. These findings support the hypothesis that FGF8 operates as a classic diffusible morphogen, establishing positional values along the A/P axis of the neocortical primordium. Additional findings indicate that the anterior source of FGF8 and FGF17 is an integral patterning center for the entire neocortex. Not supported are alternative models, in which, for example, FGF8 primarily controls development of anterior neocortex, patterning posterior neocortex indirectly through interactions with other secreted signaling molecules.

Downstream of FGF8

Transcription factors responsive to FGF8 are already implicated in neocortical area patterning (Mallamaci and Stoykova, 2006; O'Leary et al., 2007). *Emx2* is downregulated by FGF8 and promotes the development of posterior neocortical areas (Bishop et al., 2000; Hamasaki et al., 2004). FGF8 also downregulates *Nr2f1* (Sansom et al., 2005), and of the known mechanisms that mediate FGF8 signaling, this has the most striking consequences for area patterning. *Nr2f1* expression defines a comparatively sharply bounded domain in the posterior neocortical primordium (Rash and Grove, 2006). Conditional deletion of *Nr2f1* in cortex causes primary sensory areas to shrink, making way for a vastly expanded anterior cortex (Armentano et al., 2007; Faedo et al., 2008). Both *Emx2* and *Nr2f1* are upregulated by bone morphogenetic protein and Wnt signaling, originating in the mouse from the posteromedial cortical hem (Dominguez and Rakic, 2008; Ohkubo et al., 2002; Theil et al., 2002). Still missing from the picture, however, are FGF8-responsive, positive regulators of anterior and central area fates. The switch from a central to a more posterior fate when FGF8 signaling is inhibited by *dnFgfr3c* electroporation implies the existence of such positive regulators, as does the ability of ectopic FGF8 to induce duplicate somatosensory barrelfields, a central area fate, in posterior neocortex (Fukuchi-Shimogori and Grove, 2001). Genes expressed in gradients in the neocortical primordium have been found (Sansom et al., 2005), but FGF8-responsive genes that are regionally expressed at the particular time when area patterning is initiated have not yet been sought.

Integrating FGF8 levels and time of exposure

Fate-mapping experiments demonstrated that most neocortical progenitor cells do not belong to the *Fgf8* lineage. Progenitors of ventromedial prefrontal cortex are exceptional, however, lying inside the anterior FGF8 source. These cells may be specified to generate ventromedial prefrontal cortex in response to both high levels of FGF8 and prolonged exposure to FGF8. The process of integrating morphogen concentration with time of morphogen exposure to arrive at a specific cell fate has been described previously in the limb (Harfe et al., 2004; Tabin and McMahon, 2008). Sonic hedgehog (Shh), produced by the zone of polarizing activity (ZPA) in the limb bud, induces the orderly A/P array of digits (Riddle et al., 1993). In mice, cells inside the ZPA generate digits 5 and 4, whereas digit 2 and part of 3 develop in response to a Shh gradient outside the ZPA. Both 5 and 4 are exposed to the maximum level of Shh, but are distinguished because cells that spend the longest time in the ZPA generate digit 5 (Harfe et al., 2004; Tabin and McMahon, 2008). Given that *Fgf17* is expressed in a larger domain than *Fgf8*, a substantial region of prefrontal cortex may derive from progenitors inside the FGF8/FGF17 patterning source. Previous findings indicate that FGF17 is required for specification of dorsal, but not ventromedial, prefrontal cortex (Cholfin and Rubenstein, 2007). An appealing model is that area specification in prefrontal cortex is controlled by the cellular integration of FGF8 and FGF17 levels together with the time of exposure to each FGF. This model can be explored by fate-mapping experiments that follow the *Fgf8* and *Fgf17* lineages as the neocortex develops.

Patterning human neocortex

A working assumption is that mechanisms that pattern the cerebral cortex in the mouse will have a similar function in other mammals, including humans. For example, the cortical hem signaling center in the mouse generates Wnt proteins and bone morphogenetic proteins (BMPs) (Furuta et al., 1997; Grove et al., 1998), and is an organizer for the hippocampus (Mangale et al., 2008). At least by Wnt and BMP gene expression, and position next to the hippocampal primordium, the cortical hem has a human analog (Abu-Khalil et al., 2004). Moreover, human cortical abnormalities associated with faulty FGF8 or FGFR3 signaling (Frank et al., 2002; Hevner, 2005) suggest an FGF8 source regulates pattern and growth in the embryonic human telencephalon.

A key question is whether the same molecular mechanisms can pattern both small and large brains, given spatial constraints on the range of signaling molecule diffusion. This problem seems likely to be solved, not by adding mechanisms in large species to give morphogens vast ranges of action, but rather by keeping the primordia universally small. At 35 days of gestation, for example, the human neocortical primordium is at a developmental stage equivalent to E10 in the mouse, and is about 0.5 mm long (Copp, 2005), close to the size of the E10 mouse neocortical primordium, and, according to the present study, within the diffusion range of FGF8. Thus, the neocortex of the mouse and human, which differ 1000-fold in final surface area, may be patterned by the same signaling mechanisms because, at the appropriate stage of development, their primordia are similar in size.

Acknowledgements

We thank Vytas Bindokas (Director, BSD Light Microscopy Core Facility) for his assistance with confocal microscopy and data analysis, and members of the Grove and Ragsdale laboratories for their advice and comments on the manuscript. This work was supported by a grant from NIH, RO1 HD42330 (E.A.G.), and by an individual Ruth L. Kirschstein National Research Service Award to J. Wilcoxon. Deposited in PMC for release after 12 months.

Competing interests statement
The authors declare no competing financial interests.

Supplementary material
Supplementary material for this article is available at
http://dev.biologists.org/lookup/suppl/doi:10.1242/dev.055392/-/DC1

References

Abu-Khalil, A., Fu, L., Grove, E. A., Zecevic, N. and Geschwind, D. H. (2004). Wnt genes define distinct boundaries in the developing human brain: implications for human forebrain patterning. *J. Comp. Neurol.* **474**, 276-288.
Agarwala, S., Sanders, T. A. and Ragsdale, C. W. (2001). Sonic hedgehog control of size and shape in midbrain pattern formation. *Science* **291**, 2147-2150.
Altman, J. and Bayer, S. A. (1995). *Atlas of Prenatal Rat Brain Development*. Boca Raton: CRC Press.
Ashwell, K. W. S. and Paxinos, G. (2008). *Atlas of the Developing Rat Nervous System*. New York: Elsevier.
Amaya, E., Musci, T. J. and Kirschner, M. W. (1991). Expression of a dominant negative mutant of the FGF receptor disrupts mesoderm formation in Xenopus embryos. *Cell* **66**, 257-270.
Aoto, K., Nishimura, T., Eto, K. and Motoyama, J. (2002). Mouse GLI3 regulates Fgf8 expression and apoptosis in the developing neural tube, face, and limb bud. *Dev. Biol.* **251**, 320-332.
Armentano, M., Chou, S. J., Tomassy, G. S., Leingartner, A., O'Leary, D. D. and Studer, M. (2007). COUP-TFI regulates the balance of cortical patterning between frontal/motor and sensory areas. *Nat. Neurosci.* **10**, 1277-1286.
Bachler, M. and Neubuser, A. (2001). Expression of members of the Fgf family and their receptors during midfacial development. *Mech. Dev.* **100**, 313-316.
Bishop, K. M., Goudreau, G. and O'Leary, D. D. (2000). Regulation of area identity in the mammalian neocortex by Emx2 and Pax6. *Science* **288**, 344-349.
Borello, U., Cobos, I., Long, J. E., McWhirter, J. R., Murre, C. and Rubenstein, J. L. (2008). FGF15 promotes neurogenesis and opposes FGF8 function during neocortical development. *Neural Dev.* **3**, 17.
Cholfin, J. A. and Rubenstein, J. L. (2007). Patterning of frontal cortex subdivisions by Fgf17. *Proc. Natl. Acad. Sci. USA* **104**, 7652-7657.
Cholfin, J. A. and Rubenstein, J. L. (2008). Frontal cortex subdivision patterning is coordinately regulated by Fgf8, Fgf17, and Emx2. *J. Comp. Neurol.* **509**, 144-155.
Cobb, M. H. and Goldsmith, E. J. (1995). How MAP kinases are regulated. *J. Biol. Chem.* **270**, 14843-14846.
Cobos, I., Shimamura, K., Rubenstein, J. L., Martinez, S. and Puelles, L. (2001). Fate map of the avian anterior forebrain at the four-somite stage, based on the analysis of quail-chick chimeras. *Dev. Biol.* **239**, 46-67.
Copp, A. J. (2005). Neurulation in the cranial region-normal and abnormal. *J. Anat.* **207**, 623-635.
Crick, F. (1970). Diffusion in embryogenesis. *Nature* **225**, 420-422.
Crossley, P. H. and Martin, G. R. (1995). The mouse Fgf 8 gene encodes a family of polypeptides and is expressed in regions that direct outgrowth and patterning in the developing embryo. *Development* **121**, 439-451.
Dominguez, M. H. and Rakic, P. (2008). Neuroanatomy of the FGF system. *J. Comp. Neurol.* **509**, 141-143.
Driever, W. and Nusslein-Volhard, C. (1988). The bicoid protein determines position in the Drosophila embryo in a concentration-dependent manner. *Cell* **54**, 95-104.
Dubrulle, J. and Pourquie, O. (2004). fgf8 mRNA decay establishes a gradient that couples axial elongation to patterning in the vertebrate embryo. *Nature* **427**, 419-422.
Echelard, Y., Epstein, D. J., St-Jacques, B., Shen, L., Mohler, J., McMahon, J. A. and McMahon, A. P. (1993). Sonic hedgehog, a member of a family of putative signaling molecules, is implicated in the regulation of CNS polarity. *Cell* **75**, 1417-1430.
Ericson, J., Muhr, J., Placzek, M., Lints, T., Jessell, T. M. and Edlund, T. (1995). Sonic hedgehog induces the differentiation of ventral forebrain neurons: a common signal for ventral patterning within the neural tube. *Cell* **81**, 747-756.
Faedo, A., Tomassy, G. S., Ruan, Y., Teichmann, H., Krauss, S., Pleasure, S. J., Tsai, S. Y., Tsai, M. J., Studer, M. and Rubenstein, J. L. (2008). COUP-TFI coordinates cortical patterning, neurogenesis, and laminar fate and modulates MAPK/ERK, AKT, and beta-catenin signaling. *Cereb. Cortex* **18**, 2117-2131.
Frank, D. U., Fotheringham, L. K., Brewer, J. A., Muglia, L. J., Tristani-Firouzi, M., Capecchi, M. R. and Moon, A. M. (2002). An Fgf8 mouse mutant phenocopies human 22q11 deletion syndrome. *Development* **129**, 4591-4603.
Fukuchi-Shimogori, T. and Grove, E. A. (2001). Neocortex patterning by the secreted signaling molecule FGF8. *Science* **294**, 1071-1074.
Fukuchi-Shimogori, T. and Grove, E. A. (2003). Emx2 patterns the neocortex by regulating FGF positional signaling. *Nat. Neurosci.* **6**, 825-831.
Furuta, Y., Piston, D. W. and Hogan, B. L. (1997). Bone morphogenetic proteins (BMPs) as regulators of dorsal forebrain development. *Development* **124**, 2203-2212.
Garel, S., Huffman, K. J. and Rubenstein, J. L. R. (2003). Molecular regionalization of the neocortex is disrupted in Fgf8 hypomorphic mutants. *Development* **130**, 1903-1914.
Genove, G., Glick, B. S. and Barth, A. L. (2005). Brighter reporter genes from multimerized fluorescent proteins. *Biotechniques* **39**, 814, 816, 818.
Green, J. (2002). Morphogen gradients, positional information, and Xenopus: interplay of theory and experiment. *Dev. Dyn.* **225**, 392-408.
Green, J. B. and Smith, J. C. (1990). Graded changes in dose of a Xenopus activin A homologue elicit stepwise transitions in embryonic cell fate. *Nature* **347**, 391-394.
Green, J. B., New, H. V. and Smith, J. C. (1992). Responses of embryonic Xenopus cells to activin and FGF are separated by multiple dose thresholds and correspond to distinct axes of the mesoderm. *Cell* **71**, 731-739.
Grove, E. A. and Fukuchi-Shimogori, T. (2003). Generating the cerebral cortical area map. *Annu. Rev. Neurosci.* **26**, 355-380.
Grove, E. A., Kirkwood, T. B. and Price, J. (1992). Neuronal precursor cells in the rat hippocampal formation contribute to more than one cytoarchitectonic area. *Neuron* **8**, 217-229.
Grove, E. A., Tole, S., Limon, J., Yip, L. and Ragsdale, C. W. (1998). The hem of the embryonic cerebral cortex is defined by the expression of multiple Wnt genes and is compromised in Gli3-deficient mice. *Development* **125**, 2315-2325.
Hamasaki, T., Leingartner, A., Ringstedt, T. and O'Leary, D. D. (2004). EMX2 regulates sizes and positioning of the primary sensory and motor areas in neocortex by direct specification of cortical progenitors. *Neuron* **43**, 359-372.
Harfe, B. D., Scherz, P. J., Nissim, S., Tian, H., McMahon, A. P. and Tabin, C. J. (2004). Evidence for an expansion-based temporal Shh gradient in specifying vertebrate digit identities. *Cell* **118**, 517-528.
Hevner, R. F. (2005). The cerebral cortex malformation in thanatophoric dysplasia: neuropathology and pathogenesis. *Acta Neuropathol. (Berl.)* **110**, 208-221.
Krubitzer, L. (1995). The organization of neocortex in mammals: are species differences really so different? *Trends Neurosci.* **18**, 408-417.
Lander, A. D., Nie, Q. and Wan, F. Y. (2002). Do morphogen gradients arise by diffusion? *Dev. Cell* **2**, 785-796.
Liem, K. F., Jr, Tremml, G., Roelink, H. and Jessell, T. M. (1995). Dorsal differentiation of neural plate cells induced by BMP-mediated signals from epidermal ectoderm. *Cell* **82**, 969-979.
Long, F., Peng, H., Liu, X., Kim, S. K. and Myers, E. (2009). A 3D digital atlas of C. elegans and its application to single-cell analyses. *Nat. Methods* **6**, 667-672.
MacArthur, C. A., Lawshe, A., Xu, J., Santos-Ocampo, S., Heikinheimo, M., Chellaiah, A. T. and Ornitz, D. M. (1995). FGF-8 isoforms activate receptor splice forms that are expressed in mesenchymal regions of mouse development. *Development* **121**, 3603-3613.
Mackarehtschian, K., Lau, C. K., Caras, I. and McConnell, S. K. (1999). Regional differences in the developing cerebral cortex revealed by ephrin-A5 expression. *Cereb. Cortex* **9**, 601-610.
Mallamaci, A. and Stoykova, A. (2006). Gene networks controlling early cerebral cortex arealization. *Eur. J. Neurosci.* **23**, 847-856.
Mangale, V. S., Hirokawa, K. E., Satyaki, P. R., Gokulchandran, N., Chikbire, S., Subramanian, L., Shetty, A. S., Martynoga, B., Paul, J., Mai, M. V. et al. (2008). Lhx2 selector activity specifies cortical identity and suppresses hippocampal organizer fate. *Science* **319**, 304-309.
Maruoka, Y., Ohbayashi, N., Hoshikawa, M., Itoh, N., Hogan, B. L. and Furuta, Y. (1998). Comparison of the expression of three highly related genes, Fgf8, Fgf17 and Fgf18, in the mouse embryo. *Mech. Dev.* **74**, 175-177.
Mason, I. (2007). Initiation to end point: the multiple roles of fibroblast growth factors in neural development. *Nat. Rev. Neurosci.* **8**, 583-596.
Miyashita-Lin, E. M., Hevner, R., Wassarman, K. M., Martinez, S. and Rubenstein, J. L. (1999). Early neocortical regionalization in the absence of thalamic innervation. *Science* **285**, 906-909.
Moon, A. M. and Capecchi, M. R. (2000). Fgf8 is required for outgrowth and patterning of the limbs. *Nat. Genet.* **26**, 455-459.
Nagai, T., Ibata, K., Park, E. S., Kubota, M., Mikoshiba, K. and Miyawaki, A. (2002). A variant of yellow fluorescent protein with fast and efficient maturation for cell-biological applications. *Nat. Biotechnol.* **20**, 87-90.
Nauta, W. J. H. and Feirtag, M. (1986). *Fundamental Neuroanatomy.* New York: WH Freeman and Company.
Niehrs, C. and Meinhardt, H. (2002). Modular feedback. *Nature* **417**, 35-36.
O'Leary, D. D., Chou, S. J. and Sahara, S. (2007). Area patterning of the mammalian cortex. *Neuron* **56**, 252-269.
Ohkubo, Y., Chiang, C. and Rubenstein, J. L. (2002). Coordinate regulation and synergistic actions of BMP4, SHH and FGF8 in the rostral prosencephalon regulate morphogenesis of the telencephalic and optic vesicles. *Neuroscience* **111**, 1-17.
Ornitz, D. M. and Itoh, N. (2001). Fibroblast growth factors. *Genome Biol.* **2**, Reviews 3005.1-3005.12.
Ornitz, D. M., Xu, J., Colvin, J. S., McEwen, D. G., MacArthur, C. A., Coulier, F., Gao, G. and Goldfarb, M. (1996). Receptor specificity of the fibroblast growth factor family. *J. Biol. Chem.* **271**, 15292-15297.
Raballo, R., Rhee, J., Lyn-Cook, R., Leckman, J. F., Schwartz, M. L. and Vaccarino, F. M. (2000). Basic fibroblast growth factor (Fgf2) is necessary for

cell proliferation and neurogenesis in the developing cerebral cortex. *J. Neurosci.* **20**, 5012-5023.
Rakic, P. (1988). Specification of cerebral cortical areas. *Science* **241**, 170-176.
Rash, B. G. and Grove, E. A. (2006). Area and layer patterning in the developing cerebral cortex. *Curr. Opin. Neurobiol.* **16**, 25-34.
Riddle, R. D., Johnson, R. L., Laufer, E. and Tabin, C. (1993). Sonic hedgehog mediates the polarizing activity of the ZPA. *Cell* **75**, 1401-1416.
Rubenstein, J. L., Anderson, S., Shi, L., Miyashita-Lin, E., Bulfone, A. and Hevner, R. (1999). Genetic control of cortical regionalization and connectivity. *Cereb. Cortex* **9**, 524-532.
Sanchez-Arrones, L., Ferran, J. L., Rodriguez-Gallardo, L. and Puelles, L. (2009). Incipient forebrain boundaries traced by differential gene expression and fate mapping in the chick neural plate. *Dev. Biol.* **335**, 43-65.
Sansom, S. N., Hebert, J. M., Thammongkol, U., Smith, J., Nisbet, G., Surani, M. A., McConnell, S. K. and Livesey, F. J. (2005). Genomic characterisation of a Fgf-regulated gradient-based neocortical protomap. *Development* **132**, 3947-3961.
Schlessinger, J. (2000). Cell signaling by receptor tyrosine kinases. *Cell* **103**, 211-225.
Scholpp, S. and Brand, M. (2004). Endocytosis controls spreading and effective signaling range of Fgf8 protein. *Curr. Biol.* **14**, 1834-1841.
Shaner, N. C., Campbell, R. E., Steinbach, P. A., Giepmans, B. N., Palmer, A. E. and Tsien, R. Y. (2004). Improved monomeric red, orange and yellow fluorescent proteins derived from Discosoma sp. red fluorescent protein. *Nat. Biotechnol.* **22**, 1567-1572.
Shimogori, T. and Grove, E. A. (2005). Fibroblast growth factor 8 regulates neocortical guidance of area-specific thalamic innervation. *J. Neurosci.* **25**, 6550-6560.
Shimogori, T. and Ogawa, M. (2008). Gene application with in utero electroporation in mouse embryonic brain. *Dev. Growth Differ.* **50**, 499-506.
Storm, E. E., Rubenstein, J. L. and Martin, G. R. (2003). Dosage of Fgf8 determines whether cell survival is positively or negatively regulated in the developing forebrain. *Proc. Natl. Acad. Sci. USA* **100**, 1757-1762.
Sur, M. and Rubenstein, J. L. (2005). Patterning and plasticity of the cerebral cortex. *Science* **310**, 805-810.
Tabin, C. J. and McMahon, A. P. (2008). Developmental biology. Grasping limb patterning. *Science* **321**, 350-352.
Theil, T., Aydin, S., Koch, S., Grotewold, L. and Ruther, U. (2002). Wnt and Bmp signalling cooperatively regulate graded Emx2 expression in the dorsal telencephalon. *Development* **129**, 3045-3054.
Theiler, K. (1989). *The House Mouse*. New York: Springer-Verlag.
Tsang, M. and Dawid, I. B. (2004). Promotion and attenuation of FGF signaling through the Ras-MAPK pathway. *Sci. STKE* **2004**, pe17.
Wolpert, L. (1969). Positional information and the spatial pattern of cellular differentiation. *J. Theor. Biol.* **25**, 1-47.
Wolpert, L. (1996). One hundred years of positional information. *Trends Genet.* **12**, 359-364.
Xu, J., Liu, Z. and Ornitz, D. M. (2000). Temporal and spatial gradients of Fgf8 and Fgf17 regulate proliferation and differentiation of midline cerebellar structures. *Development* **127**, 1833-1843.
Yu, S. R., Burkhardt, M., Nowak, M., Ries, J., Petrasek, Z., Scholpp, S., Schwille, P. and Brand, M. (2009). Fgf8 morphogen gradient forms by a source-sink mechanism with freely diffusing molecules. *Nature* **461**, 533-536.
Yun, M. E., Johnson, R. R., Antic, A. and Donoghue, M. J. (2003). EphA family gene expression in the developing mouse neocortex: regional patterns reveal intrinsic programs and extrinsic influence. *J. Comp. Neurol.* **456**, 203-216.
Zhang, X., Ibrahimi, O. A., Olsen, S. K., Umemori, H., Mohammadi, M. and Ornitz, D. M. (2006). Receptor specificity of the fibroblast growth factor family. The complete mammalian FGF family. *J. Biol. Chem.* **281**, 15694-15700.